Australasian Universities Power Engineering Conference (AUPEC 2004)
26-29 September 2004, Brisbane, Australia

INVESTIGATION OF THE BEHAVIOUR OF AN AVR IN A BALLAST LOAD FREQUENCY CONTROLLED STAND ALONE MICRO-HYDROELECTRIC SYSTEM

R. Jarman and P. Bryce

Faculty of Engineering
University of Technology, Sydney

Abstract

Extensive field experience in micro-hydroelectric systems in remote rural communities demonstrates the use of a typical Automatic Voltage Regulator (AVR) supplied as with a synchronous alternator can be the cause of unsatisfactory system performance. This paper presents the published evidence, and verifies it with measured results from a full scale micro-hydroelectric test rig. Anecdotal advice suggesting the cause of instability results from the response of the two competing feedback control systems (the ballast load frequency controller and the AVR) is verified. System modelling also confirms the Under Frequency Roll-off (UFRO) characteristic of the AVR contributes significantly to unsatisfactory performance.

1. INTRODUCTION

Hydroelectricity as an untapped resource concentrated in the 'South' nations, is an important technology for addressing energy poverty and its ramifications for global equity. Smaller-scale hydroelectricity, with minimal to no water storage, can provide opportunities for poverty reduction [1] with 48 000 medium to small units now in place serving 300 million residents in China alone.

Extensive field experience in stand alone micro-hydroelectric systems [2] demonstrates the use of a typical Automatic Voltage Regulator (AVR) as supplied with a synchronous alternator can be the cause of unsatisfactory system performance.

This paper reviews the observations of the instability, verifies them with measured results from a full scale micro-hydroelectric test rig (Figure 1) and presents arguments suggesting the cause is related to the similar time constants of the two feedback systems as well as the Under Frequency Roll-Off (UFRO) characteristic of the automatic voltage regulation (AVR).

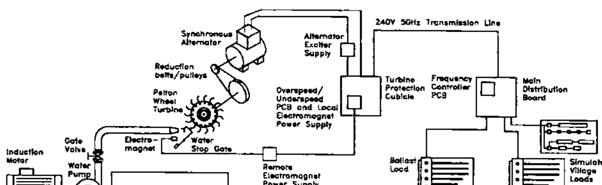

Figure 1 - Main system components of the UTS micro-hydroelectric test rig in the Renewable Energy Laboratory

2. BALLAST LOAD FREQUENCY CONTROLLED MICRO-HYDROELECTRIC SYSTEM

In a typical APACE VFEG* micro-hydroelectric system (generating capacity < 100kW), electricity is generated at $240V_{AC}$ 50Hz via a standard off-the-shelf brushless self excited synchronous alternator. These run-of-the-river schemes convert the kinetic energy of falling water to rotational energy via a pelton wheel or cross flow water turbine. System speed (ω_m) and hence frequency (f) is regulated by balancing the system torque equation at a nominal set-point speed – typically 1500RPM for a 4 pole alternator.

$$T_{shaft} - T_{load} = T_{inertia} = J\frac{d\omega_m}{dt} \quad \text{[Nm]} \qquad (1)$$

The turbine supplies the shaft torque to the alternator, the opposing load torque is made up of the alternator electromagnetic torque and system losses. The system rotational inertia (J) is in the order of 0.55 kgm^2 for a typical 40kW system.

A ballast load frequency controller switches resistive load (ballast) to increase or decrease electromagnetic torque, regulating shaft speed, and hence system frequency. Variations in system frequency as a result of changes in consumer demand as well as long term seasonal variations in water supply are accounted for in the controller algorithm.

The alternator AVR is replaced with a fixed (but user adjustable) field current derived from a linear power supply circuit, based on a typical transformer, bridge rectifier and linear regulator circuit. System voltage is then proportional to frequency, and regulated by the frequency controller.

3. SUMMARY OF LITERATURE

Excitation requirements for synchronous machines in these systems is not as simple as first thought [3]. Published [4] and observed [5, 6] evidence suggests it is nearly impossible to get an AVR excited machine to steady state, and this is confirmed from the practical implications of bringing the alternator up to running speed described by the AVR manufacturer [7].

AVR's are a common pitfall in micro-hydroelectric systems. They are designed for use in diesel genset systems only, and afford extremely poor reliability in hydro systems due to current boosting at low operating speeds, although a solution may lie in appropriate component specification [8, 9].

Unstable operation with load changes have been predicted [10], the interaction between load controller and AVR has been considered the source of instability, and one solution found by 'dumbing down' the controller [11]. Also considered was the suggestion that two stable operating points may exist for the one turbine opening as an explanation for an observed 45-55Hz instability (or hunting) [4].

Predictions of a minimum system inertia requirement for stable operation (around 3.2kgm^2 for a 40kW system) have been made [12, 13]. Some designers [14, 15, 16, 17] added flywheels to the alternator shafts to overcome instability, and then went on to develop various rationale to explain why or how it works. As a comparison, the rotational inertia for a typical 40kW diesel engine driven system is around 4.5kgm^2 [18].

4. EXPERIMENTAL VERIFICATION OF INSTABILITY

Experimental tests were undertaken to measure and record various parameters as the system became unstable. Figure 2 compares the graphs for an increase and then decrease in water power; the graphs on the left hand side show the system with fixed excitation and ballast load controller, on the right show the system with AVR controlled excitation and ballast load controller.

A gate valve is used to vary water power input to the turbine and results in a near linear relationship between water head and flow; a water head input of around 15 metres (flow = 12 litres/sec) establishes a steady state operating point where the system losses and electrical excitation balances the water power input.

Significant points for the fixed excitation graphs include: the shape of the alternator current is the same as the water head (since system voltage remains near constant, and electrical power balances water power input); the ballast load frequency controller maintains system frequency at about 50Hz; terminal voltage drops with increase load on the alternator as expected. Significant points for the AVR controlled graphs include: the AVR increases field current with increase load on the alternator; unstable oscillations in system frequency increase in amplitude; at the point where the oscillations in system frequency are a maximum, each transit below 45Hz results in an immediate reduction in terminal voltage; the oscillations can only be reduced by shutting the system down.

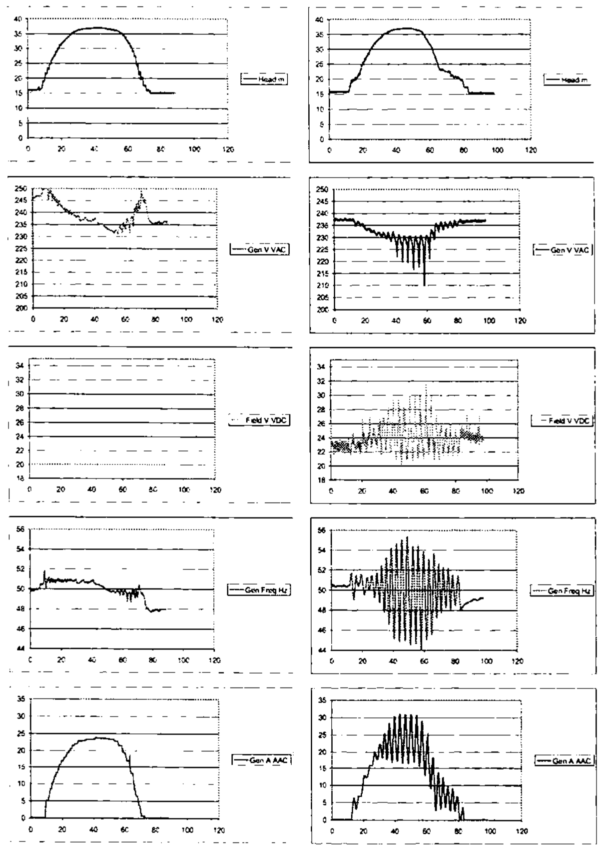

Figure 2 - Graphs comparing the response of various system parameters versus time [sec] for an increase and decrease in hydro power (water head)

5. SYSTEM MODELLING

Modelling of the hydraulic system components yields the expected parabolic shape of the power versus speed curve [19]. Figure 3 graphs the measured locus of steady state operating points as a six element binary weighted load resistance was switched in 64 discrete steps. The graph includes the transients from four of the larger step changes in this process.

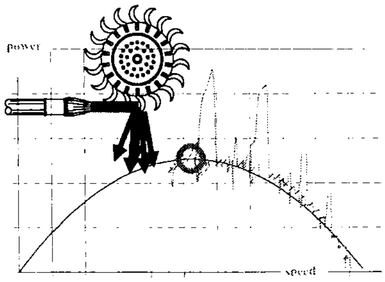

Figure 3 – Experimental determination of the turbine power versus speed curve

Varying the water input results in a set of (ideal) parabolic curves representing steady state operating points for the system. These curves give rise to the turbine speed versus torque characteristic shown in Figure 4, although only a limited range [$125<\omega_m<189$ rad/sec] of these curves is considered representative for modelling purposes.

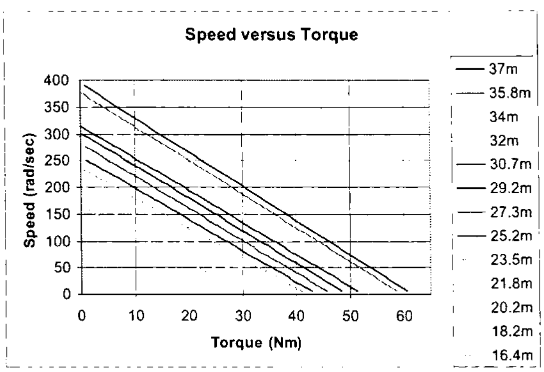

Figure 4 - Speed (angular velocity) versus load torque for various water head input

Modelling of the electrical system components yields an equivalent first order representation of the alternator shown in Figure 5.

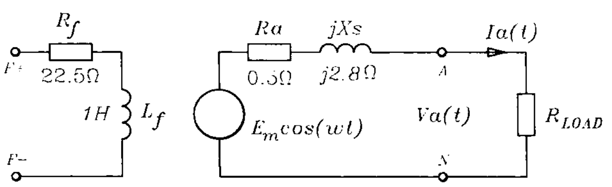

Figure 5 - Electrical circuit representation of the (equivalent) single phase brushless self excited synchronous alternator

Analysis of off-the-shelf AVR's verified the under frequency roll-off characteristic (UFRO). In diesel genset applications, when a large load is applied to the alternator resulting in significant speed reduction, the UFRO characteristic reduces system excitation, and hence terminal voltage and electromagnetic torque. This affords the diesel engine governing system opportunity to recover nominal speed.

This feature is user settable, the shaded region in Figure 6 shows a typical region of operation for an AVR resulting in reduced output from the alternator as a function of frequency.

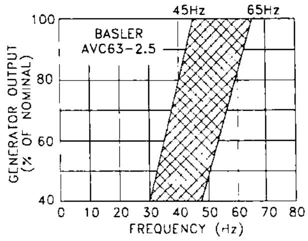

Figure 6 - Graph of Under Frequency Roll-off characteristic for a Basler AVC63-2.5 AVR

6. EQUATIONS FOR INDUCED VOLTAGE

Faraday's Law yields the induced voltage:

$$E_{RMS} = 4.44 f N \phi \qquad [2]$$

and Kirchhoff's Laws yield the expression:

$$E_{RMS} = I_a(R_a + jX_S) + I_a R_{LOAD} \qquad [3]$$

where $R_{LOAD} = R_{VILLAGE} + R_{BALLAST}$

Equating the expressions affords insight into the interaction between the excitation control system (AVR) and ballast load frequency controller for a change in village load. From [2] and [3]:

$$\begin{aligned} E_{RMS} &= 4.44 f N \phi \\ &= I_a(R_a + jX_S + R_{VILLAGE} + R_{BALLAST}) \end{aligned} \qquad [4]$$

In the case of a hydro turbine with fixed excitation as used in the APACE VFEG micro-hydroelectric systems:

$$\begin{aligned} \underset{f(\omega_m)}{\Delta E_{RMS}} &= k_1 \underset{\tau\approx 1s}{\Delta f} \\ &= \underset{\tau\to 0}{I_a} (\underbrace{R_a + jX_S}_{unchanged} + \underbrace{\Delta R_{VILLAGE}}_{stimulus} + \underbrace{\Delta R_{BALLAST}}_{\tau\approx 60ms}) \end{aligned} \qquad [5]$$

where $k_1 = 4.44 N\phi$ and N = number of windings.

A change (*stimulus*) in village load ($\Delta R_{VILLAGE}$) will result in a near instantaneous ($\tau\to 0$) change in alternator current (ΔI_a). The change in electromagnetic torque results in a change in system frequency ($\tau\approx 1$sec) which is a function of system rotating inertia (J). The ballast load frequency controller senses this change, and responds ($\tau\approx 60$ms) accordingly to regulate system speed. Induced voltage is a function of speed (ω_m) only, since air gap flux (ϕ) is constant.

In the case of the hydro turbine with AVR controlled excitation:

$$\begin{aligned} \underset{f(\omega_m,\phi)}{\Delta E_{RMS}} &= k_3 f \underset{\tau\approx 20ms}{\Delta\phi} + k_3 \phi \underset{\tau\approx 1s}{\Delta f} \\ &= \underset{\tau\to 0}{\Delta I_a} (\underbrace{R_a + jX_S}_{unchanged} + \underset{(stimulus)}{\Delta R_{VILLAGE}} + \underset{\tau\approx 60ms}{\Delta R_{BALLAST}}) \end{aligned} \qquad [6]$$

where $k_3 = 4.44N$

In this system, induced voltage is a function of speed and air gap flux and as the time constants for the feedback elements are in the same order of magnitude, $\tau \approx$ 20ms for the AVR; $\tau \approx$ 60ms for the frequency controller, instability results.

By increasing the system rotating inertia and slowing response rate of frequency controller [16], the time constants of the two control systems are separated. The system speed components behave in a similar manner to a governed diesel prime mover:

$$\underset{f(\varpi_m,\phi)}{\Delta E_{RMS}} = k_3 f \underset{\tau\approx 20ms}{\Delta\phi} + k_3\phi \underset{\tau\approx 13s}{\Delta f}$$

$$= \underset{\tau\to 0}{\Delta I_a}(\underbrace{R_a + jX_S}_{unchanged} + \underset{(stimulus)}{\Delta R_{VILLAGE}} + \underset{\tau\approx 2s}{\Delta R_{BALLAST}}) \qquad [7]$$

7. OPERATING POINTS ON THE TURBINE POWER VERSUS SPEED CURVES

Varying the water head input yields a family of parabolic shaped curves of the turbine power versus speed characteristic. Assuming the alternator has constant excitation, a family of parabolic resistive load power curves can mapped onto the turbine power graph as shown in figure 7.

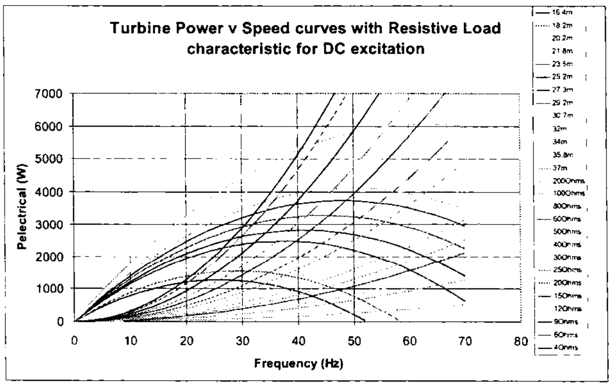

Figure 7 - Steady state electrical power versus frequency for various water head input, with various Resistive Load characteristic curves for constant DC excitation.

The intersection of a turbine and resistive load curve is a system steady state operating point. During load changes, a trajectory was measured and plotted onto these curves. Figure 8 shows a steady state operating point at (50Hz, 2000W). For the system with no ballast load frequency controller, when a 1kW load was applied, the plot shows the trajectory to the new steady state operating point at (44.5Hz, 2250W). A similar trajectory is shown for the load rejection transient.

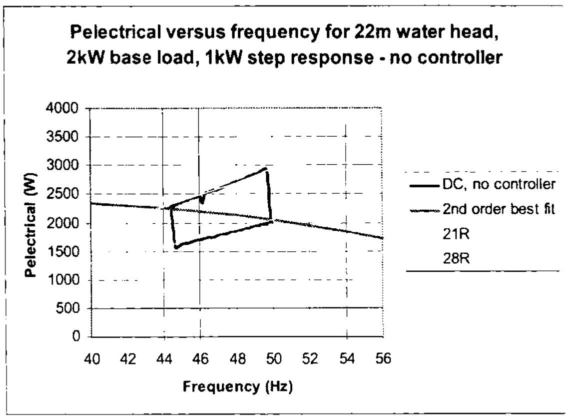

Figure 8 - Trajectory for $P_{electrical}$ during load application and rejection for fixed excited system with no controller.

Figure 9 shows the system response with the ballast load frequency controller. When a 1kW load was applied, the figure shows the trajectory as the controller returns the system to the nominal (50Hz) operating point. Note the load controller response was less than optimal during these tests, and hence the response appears underdamped.

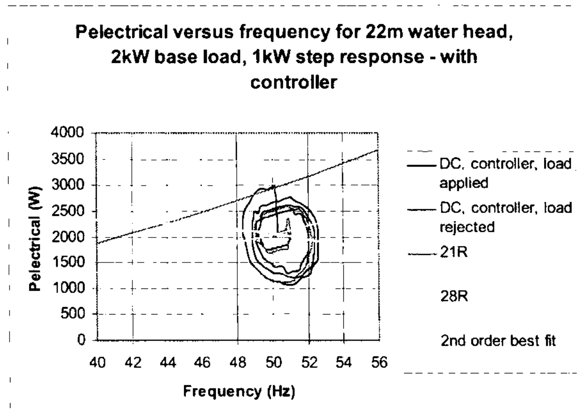

Figure 9 - Trajectory for $P_{electrical}$ during load application and rejection for fixed excited system with ballast load controller.

In comparison, an AVR controlled excitation yielded a significantly different set of resistive load power curves on the turbine curves. These are shown in figure 10.

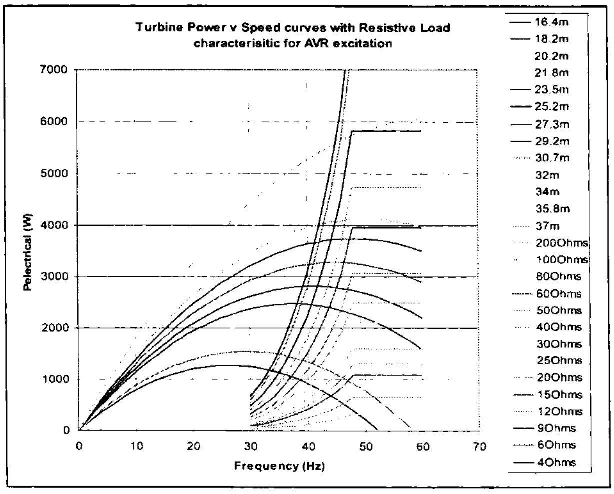

Figure 10 - Steady state electrical power versus frequency for various water head input, with various Resistive Load characteristic curves for AVR controlled excitation.

The flat part of the curves results from the impact of maintaining constant terminal voltage, and hence power. The roll-off characteristic in this theoretical model was set at 47Hz and excitation is reduced according to the graphs shown in Figure 6. In practice, the UFRO can be adjusted, a typically factory setting is around 45-46Hz.

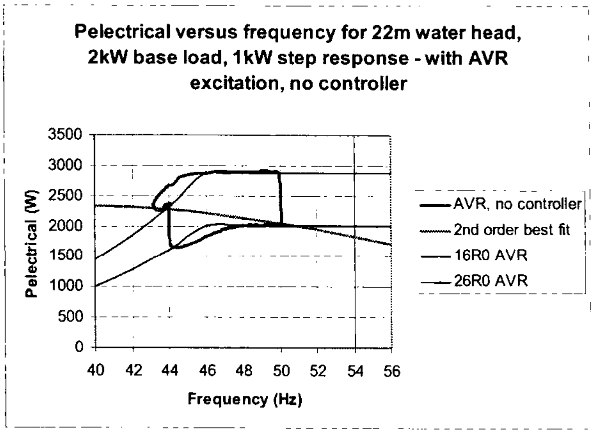

Figure 11 - Trajectory for $P_{electrical}$ during load application and rejection for AVR excited system with no controller.

Figure 11 plots a measured trajectory over a parabolic turbine power speed curve, and theoretical resistive power curves for AVR with UFRO set at 46Hz. A steady state operating point exists at (50Hz, 2000W). For the system with no ballast load frequency controller, when a 1kW load is applied, the trajectory plots the path to the new steady state operating point at (44Hz, 2300W). Note that the system power remains approximately constant until the system speed reaches the 45Hz UFRO set point. A similar trajectory is shown for the load rejection transient.

8. OPERATING ON THE NEGATIVE OR POSITIVE SIDE OF THE TURBINE POWER CURVE

Operating on the negative slope of the power speed curve will result in a trajectory towards new steady state operating point which opposes the change in demand, and will therefore assist speed regulation. However, the change in speed over this trajectory for an AVR excited system is faster than the fixed DC excited system.

Operating on the positive slope will result in a trajectory towards a new steady state operating point which, in the case of an increase in demand, cannot be sustained, and will therefore hinder speed regulation action. As a result, an AVR excited systems cannot be brought to a steady state condition; ie. it is not possible to bring the system up to a nominal speed as is the case with an externally governed system such as a diesel engine prime mover [7].

From observations of the system operating on either slope, it is evident that the AVR readily 'drops into' the UFRO condition, and tends to stay there in a reduced excitation stable operating condition. Where installed, a ballast load controller will respond to this low frequency operating point by reducing ballast load. But the return trajectory out of the UFRO condition usually requires a significant change in ballast load, and as a result, the system speed increases rapidly, overshoots the nominal set-point, and the similar response rates of the load controller and AVR result in the system returning to UFRO condition.

9. CONCLUSION

The observations of unsatisfactory performance and instability in micro-hydroelectric systems resulting from the interaction of the ballast load frequency controller and automatic voltage regulators have been verified. System modelling yields analysis suggesting the similar time constants of the two feedback systems (speed and voltage) contribute to instability.

The Under Frequency Roll-Off (UFRO) characteristic results in a reduced excitation steady state operating point that AVR excited systems appear to fall into. The system frequency at this steady state operating point is not necessarily the UFRO set-point, but is dependent on hydraulic power input.

This study also yields an understanding of the possible steady state operating points on the turbine power speed curves for the constant or AVR excited systems. Constant excitation permits operation on the positive or negative slope of the curve, whilst stable operation is only possible on the negative slope side of the curve for the AVR excited system.

10. ACKNOWLEDGEMENTS

We acknowledge the continued support of the Faculty of Engineering at the University of Technology, Sydney in making further research and development work in this field possible.

* APACE VFEG is a non-profit development assistance agency, implementing micro hydroelectric schemes over the past 20 years. Further information about the APACE VFEG projects can be found at www.apace.uts.edu.au.

11. REFERENCES

[1] Bryce, P., Community Action for Renewable Energy, 2004. http://www.cru.uea.ac.uk/tiempo/floor0/archive/issue3637/t3637a5.htm (downloaded 29-4-04)

[2] Jarman, R., and Bryce, P. "Manawai Harbour micro hydroelectric scheme: a case study in appropriate technology transfer", International Small Islands Studies Association (ISISA) Conference, Isle of Skye, 16-20 October, 2000.

[3] Chehu F., and Kohler, R., "Control system for mini hydro plants", Water Power and Dam Construction, January 1989, pp25-26.

[4] Fischer, G., Arter, A., Meier, U., and Chapallaz, J.M., "Harnessing Water power on a Small Scale, Volume 8, Governor Product Information", SKAT Swiss Centre for Appropriate technology, St.Gallen, 1990.

[5] Correspondence with Peter Lynch, Pelena Pty Ltd, peterlynch@pelena.com.au

[6] Correspondence with Paul Bryce, Technical Manager, APACE VFEG, Sydney, paulb@eng.uts.edu.au

[7] Newage International, "SA465 Automatic Voltage Regulator (AVR) Specification, Installation and Adjustments", Newage International Limited, Stamford, 2000.

[8] Harvey, A., "Micro-hydro design manual – A guide to small-scale water power schemes", Intermediate Technology Publications, London, 1993.

[9] Fraenkel, P., Paish, O., Harvey, A., Brown, A., Edwards, R., and Bokalders, V., "Micro-hydro Power, A Guide for development workers", Intermediate Technology Publications, London, 1991.

[10] Elsedawi, I. R., Elassal, A. H., and Azzouz, E. M., "Effects of AVR systems on the performance of Synchronous generators", CCECE'97 – IEEE, 1997

[11] Portegijs, J., "The humming bird electronic load controller/induction generator controller", ENECO Dutch energy distribution company, humbird.zip downloaded from www.geocities.com/wim_klunne/hydro/egroup/portegijs.html on 17 June 2001.

[12] Hagen, D.L., "Developments in controls to govern mini- and micro-hydropower systems", Renewable Energy Review Journal, Vol. 8, No. 2, December 1986.

[13] Robinson, P., and Kormilo, S., "Recent advances in the development of microcontroller based electronic load controllers", First International Conference on Small Hydro organized by International Water Power and Dam Construction, Hyatt Regency Hotel, Singapore,13-16 February, 1984.

[14] Kormilo, S., and Robinson, P., "Electronic control of small hydroelectric schemes using a microcomputer", IEE Proceedings, Vol 131, Pt E, No. 4, Jul 1984, pp. 132-136.

[15] Henderson, D., "Recent developments of an electronic load governor for micro hydroelectric generation", IEE Renewable Energy, Conference publication No. 385, 17-19 November 1993.

[16] Woodward, J.L., and Boys, J.T., "A low cost electronic load governor for energy management", First International Conference on Small Hydro organized by International Water Power and Dam Construction, Hyatt Regency Hotel, Singapore, 13-16 February, 1984.

[17] Elder, J.M., Boys, J.T., and Woodward, J.L., "Integral cycle control of stand-alone generators", IEE Proceedings, Vol 132, Pt C, No. 2, March 1985, pp57-66.

[18] Hino Motors Ltd., "Hino WO4D – Diesel Engine for Industrial use – Technical Data", Hino Motors Ltd Public relations Office, Tokyo, 2000.

[19] Thake, J., "The micro-hydro turbine manual: design, manufacture and installation for small scale hydropower", ITDG Publishing, London, 2000.